Published in Sensors and Actuators A: Physical 126, issue 1, 241-252, 2006
which should be used for any reference to this work

Matrix of 10 × 10 addressed solid propellant microthrusters: Review of the technologies

Carole Rossi [a,*], Danick Briand [b], Maxime Dumonteuil [a], Thierry Camps [a], Phuong Quyên Pham [b], Nicolaas F. de Rooij [b]

[a] *LAAS-CNRS, 7 ave du colonel Roche, 31077 Toulouse cedex 4, France*
[b] *IMT, University of Neuchâtel, Jaquet-Droz 1, P.O. Box 3, CH-2007 Neuchâtel, Switzerland*

Abstract

An EC funded MicroPyros project has permitted to develop the technologies to fabricate, assemble and command solid propellant microthrusters arrays for thrusts of a few of milli Newtons The prototype built for space application has 100 individually addressed Ø 1.5 mm × 1.5 mm thrusters on 576 mm^2. Nozzles' throats are 250 μm and 500 μm. This paper reviews the prototype structure and details the final processes for the fabrication and assembling. This paper presents also a new addressing technology based on polysilicon threshold elements used for the addressing and heating of each thruster in the array. With polysilicon threshold element, ignition success is of 100% with an input power of 250 mW using a zirconium perchlorate potassium (ZPP) material. Then, the combustion of a glycidyle azide polymer (GAP) is sustained in the chamber and generate thrusts in the range of 0.3–2.3 mN depending of the micronozzle dimension.

Keywords: MEMS; Microthruster; Microfabrication; Electrical addressing

1. Introduction

The growing interest in using microspacecraft in space industry and governmental agencies is now established. The constraints of mass, dimension, power and cost with microspacecraft arise several challenges to choose the right system and the best technology to fabricate the satellite's subsystems. One of these is the micropropulsion module to compensate the forces acting on the satellite, to realize the orbital manoeuvring and for the satellite attitude control. The precise requirements in terms of delta-V depend on the mission. For many low cost missions as earth observation or science experiment, not only are thrust level and precision requirements important for the choice of the propulsion option, but also the mass, power and the reliability will greatly influence the choice. The rules can be summarized simply as:

- The smallest and lightest will be the best.
- The power consumption must be reduced to its minimum.
- The reliability must be maximum.

In this context, solid chemical micropropulsion could represent a very interesting option for station keeping applications, some orbital manoeuvres or mechanical deployment, especially where low cost and low power consumption are key specifications. The concept and the technology for the fabrication of solid chemical microthrusters are very simple: a solid energetic material stored in a micro machined reservoir burns and the gases of combustion are accelerated through an adapted nozzle to produce a thrust. The system is flexible and could have a great potential for application in the space industry: the number of thrusters can be adapted to the number of time the propulsion system will have to be used in a specific mission while the size of the individual thruster can be tuned to obtain the required thrust force. Given these above reasons, solid chemical micropropulsion devices have been developed within research laboratories in Europe, USA and Asia and will be overviewed in Section 2.

* Corresponding author.
E-mail address: rossi@laas.fr (C. Rossi).

In Europe, the Micropyros project, born from the collaboration between the LAAS,[1] IMT,[2] IMTEK,[3] SIC,[4] ASTC,[5] and LACROIX and funded by the European Commission (IST-99-29047), proposed to develop a module of 10×10 addressed microthrusters capable of generating thrust in the range of mN s. More precisely, within Micropyros: MEMS-based robust and reliable fabrication technologies have been developed and validated for the realization of each part of the propulsion module. A polysilicon based addressing technology has been also developed to address and ignite individually each thruster. A portable electronic circuitry has been implemented to control the ignition. A full designing package has been developed to predict ignition, thrust and thermal crosstalk. Finally, characterization means including an ignition test bench, a thrust balance and a thrust vector misalignment have been set up.

The focus of this paper is to review the design and present the technologies used for the fabrication and assembling of the 10×10 addressed thrusters. The other points (modelling, electronic development and experimentations) have been or will be reported elsewhere [1–3].

2. State-of-the-art of solid chemical propulsion

LAAS has initiated the solid propellant micropropulsion concept in 1998 [4] by proposing arrays of one shot microthrusters in a three-layer sandwich configuration, electrically ignited for mN s impulses applications. A few months later, an American team made of TRW, Aerospace and Caltech published a similar micropropulsion approach “Digital Micropropulsion” [5] targeting impulses below 1 mN s. In 2004, a team from Singapore [6] presented a solid propellant microthruster technology all fabricated in a silicon wafer to produce 0.1 mN s. Since 1998, numerous papers on solid propellant micropropulsion have been published [7–13]. They are all based on the same principle: one solid energetic material stored in a chamber is heated up by means of an igniter until its ignition temperature is reached. As soon as the ignition energy and temperature are reached, the combustion starts and propagates itself through the material contained in the chamber. The hot gas generated by the combustion is then accelerated through the nozzle. The diverging part of the nozzle enables to guide the gas flow and accelerate it at the exit. They can be differentiated on four main points:

1. The type of energetic material. A couple of teams [5,7] use explosive that ensures a chemical reaction even at very tiny sizes (reservoir diameter $<600\,\mu$m). But their reaction is unstable and difficult to control, that is why other teams as Micropyros one have preferred the use of propellants.
2. Ignition location: back side or front side (gas release side). The front side ignition is the best way to have a well-established combustion process. But it requires the availability of a technology that allows the production of heating resistors on dielectric membranes, sufficiently robust to withstand the filling pressure, but also sufficiently thin to break rapidly when pressure increases [8,10,11]. Some teams find other ways as inserting wires in slots to ignite on the front side without membranes [6].
3. The size of each thruster and the density. The size depends on the targeted performances and applications: for example, in attitude control, the required thrust impulses are around 10^{-6} N s to 10^{-5} N s [5,7,9,13], whereas position maintenance and orbital maneuvers will require more powerful impulses, on the order of 10^{-5} N s to 10^{-3} N s [6,8,10,11].
4. The addressing technology. The one shot characteristic (therefore consumable) of each thruster can be compensated by the realization of arrays of individually addressable microthrusters that can be fired when needed. 2D addressing reveals technological challenges especially when high integration level is targeted. Most consists of non addressed matrixes [9–13] or stacked thrusters vectors [6] requiring the same number of electrical connexions than the number of thrusters thus limiting its application. More integrated technologies based on silicon nitride micro bridge and CMOS transistor have been proposed in [7] and the integration of silicon PN diodes have been also proposed in [8].

Micropyros propulsion module consists of a 2D addressed array of 100 $1.5\,\text{mm} \times 1.5\,\text{mm}$ solid propellant microthrusters on a $576\,\text{mm}^2$ chip area. Each microthruster has been designed to produce impulse of a few mN s. The heating and addressing elements are located at the topside of each thruster and on a thin membrane ensuring a low ignition power.

3. Review of the design, materials and technologies’ choices

3.1. Architecture and dimension

A solid propellant thruster is in general composed of a combustion chamber, an igniter and a nozzle. For the design, two different approaches are possible: the so-called planar and vertical design (cf. Fig. 1).

The vertical approach consists of a stack of several wafers to build the thruster geometry whereas the planar one contains all the thruster’s parts (nozzle, igniter and chamber) in the same wafer. In the planar design, any thruster and nozzle shapes can be realized in one micromachining step. However, the vertical design is more suitable for the realization of arrays of thrusters. In the planar approach, individual lines of thrusters would have to be stacked together to obtain a two dimensional arrays and the integration of the electronic components, such as diodes, would be more complicated for the realization of dense arrays. For these reasons, a vertical approach was chosen for the design. It

[1] Laboratoire d’Analyse et d’Architecture des Systèmes, Centre National de la Recherche Scientifique, Toulouse, France, http://www.laas.fr/.

[2] Institute of Microtechnology, University of Neuchâtel, Neuchâtel, Switzerland, http://www.unine.ch/imt/.

[3] Institute of Microsystem Technology, The Albert-Ludwigs University Freiburg, Freiburg, Germany, http://www.uni-freiburg.de/.

[4] Instrumentation and Communication Systems, University of Barcelona, Barcelona, Spain, http://www.ub.es/.

[5] Center for Advanced Microengineering, Uppsala University, Uppsala, Sweden, http://www.astc.material.uu.se/.

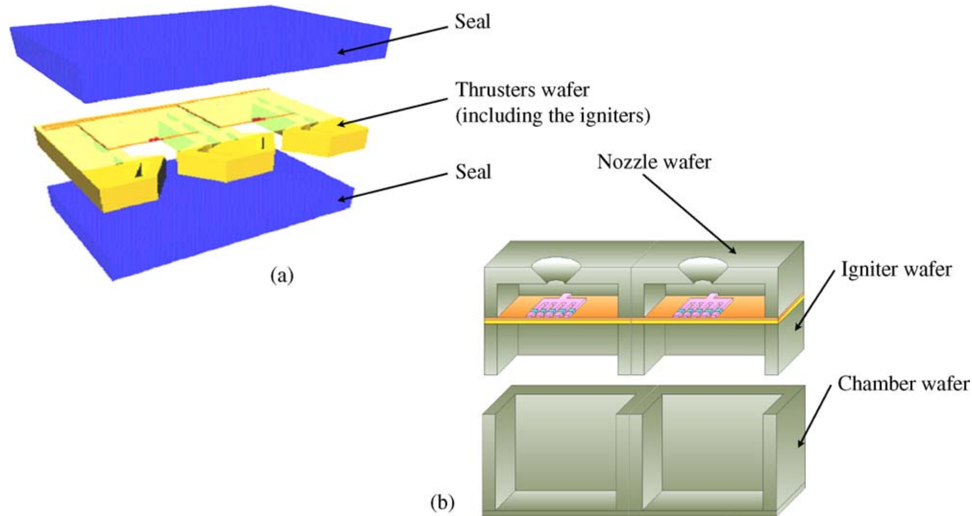

Fig. 1. Schematic view of the (a) planar and (b) vertical thruster design.

consists of four parts (see Fig. 2). The first silicon layer contains the micronozzles. The second silicon layer holds the igniters and addressing elements. The third layer, in photoetchable glass or silicon, holds the propellant reservoirs. A fourth Pyrex layer seals the device. An intermediary chamber can be added between the igniter and the propellant reservoir to have a reliable operation.

A high density of integration is ideally desired for the entire propulsion system. However, limitations appear when scaling down the dimensions due to the thermal crosstalk and combustion considerations. Most propellants, even doped with metallic charges, do not have reliable combustion below the mm^2 due to thermal losses [14]. For nanosat station keeping or de-orbit application, a previous evaluation of the thrust and total impulse has led to the design of thrusters with chamber section over the mm^2 [15]. Based on these considerations and supported by simulations performed at IMTEK [16], the chamber section of each thruster is of 1.5 mm × 1.5 mm (circular design is also possible) and the width of the nozzle throat has been calculated to be 250 μm and 500 μm, for a resulting impulse bit force of a few mN s. The pitch between two thrusters is of 2.25 mm. For silicon reservoir, the pitch is of 2.5 mm to include air groove for thermal insulation. The electronic control module is placed underneath the thruster array.

3.2. Choice of the energetic material

The choice of the energetic material influences greatly the design options and particularly the critical combustion dimensions. Two options are possible: either the use of available “safe” fairly insensitive materials such as homogenous or composite propellant, or the use of class 1:1 materials that are highly sensitive and energetic. Micropyros team has preferred the use of propellants (composite one) for three main reasons:

1. These materials sustain a stable combustion originating from an oxidation-reduction reaction when a surface has reached its ignition temperature (T_i). Rates of self-sustained combustion in these materials are relatively low, of the order of a few millimetres to a few centimetres per second as a linear phenomenon. Deflagration is only possible under very particular environmental conditions (very strong confinement and high energy input), that are impossible in small volume.

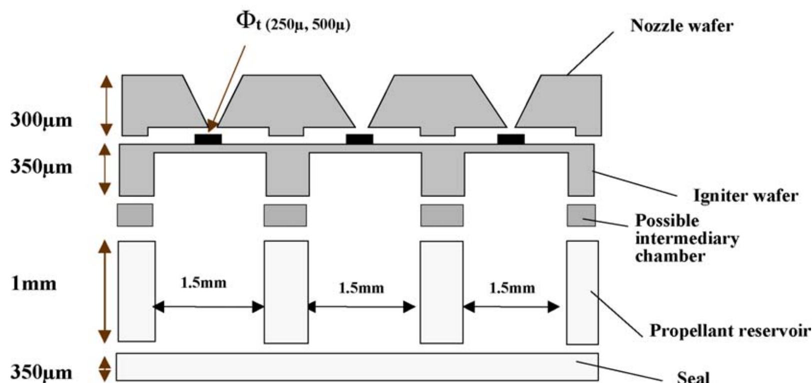

Fig. 2. Schematic view and dimensions of Micropyros thrusters’ shape.

2. They release a very large quantity of gas at high temperature that makes them particularly attractive for propulsion. The variety of ”of the shelf” propellants is very large (homogenous, simple base, double base, composite), and materials more or less adapted to the constraints of targeted applications can be formulated by adding metallic charges or changing the binder type [17–19].
3. Composite propellants have viscous physical appearance before reticulation and a solid appearance after so that a silk screen printing method can be used to deposit and fill a small cavity [20].

For Micropyros thrusters, two different propellants have been chosen: the first one is a composite propellant made with a glycidyle azide polymer mixed with ammonium perchlorate and doped with zirconium particles (called GAP in the rest of the paper). GAP is contained in the reservoir part. A more sensitive and energetic substance, zirconium perchlorate potassium (called ZPP), has been also formulated and is used in the igniter part to lower the ignition energy and have a reliable ignition.

3.3. Choice of the structural materials and technologies of fabrication

The chosen application and the vertical design approach involve technological challenges of different natures. Different parts have to be assembled together to form the complete thruster structure. These parts have to be compatible with the filling and bonding procedures and the interconnections to the external driving circuitry. Moreover, the whole device will be submitted to relatively large variations of temperature when operating in space. Therefore, the materials were evaluated based on their thermal and mechanical properties. Different materials such as silicon (monocrystalline, porous), glass (Pyrex, quartz, Foturan), ceramics and polymers were considered. A summary of the advantages and disadvantages related to some of these materials is presented in Table 1.

One main disadvantage of ceramic materials is the difficulty in the integration of electronic components. Polymers are a possible candidate to make a single shot thruster but mechanically and thermally unstable for their application in the fabrication of an integrated array of microthrusters [18]. Therefore, the processing was mainly performed on silicon and glass (Foturan) wafers, with, respectively, the advantages of a high melting point and of a low thermal conductivity, to benefit from the know-how related to the silicon technology and to ease the integration of the electronics components necessary for the addressing of the individual thrusters in the array.

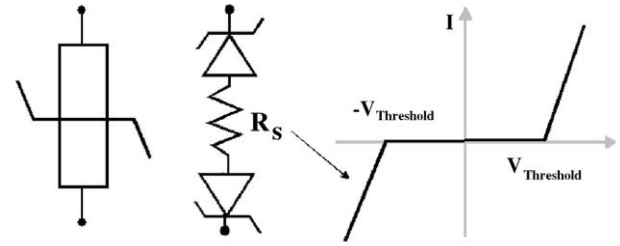

Fig. 3. Symbol, equivalent electric schema and characteristic I(V) of an elementary addressing element.

3.4. Choice of the addressing technology

We have chosen an addressing principle based on the use of polysilicon symmetrical thresholds elements for two main reasons. It permits to realize the heating and addressing functions in a single layer of polysilicon. It also permits the realization of an addressable array of heating elements with a simple process and can be implemented on bulk silicon and on suspended dielectric membrane. Fig. 3 gives the symbol, the equivalent electric components and its electrical characteristic.

$V_{Threshold}$ is the threshold voltage of an elementary thruster.

Each symmetrical threshold element consists of several Zener polysilicon diodes (P+/N+) in series as shown in Fig. 4.

The symmetry of the threshold element (cf. Fig. 3) does not permit to distinguish a forward or reverse electrical behaviour. But, we distinguish a “*blocked state*” ($I_{STE} \approx I_{Sat}$) for a voltage lower than $|V_{Threshold}|$ and a “*conductive state*” for a voltage greater than $|V_{Threshold}|$. In the conductive state, the quasi-linear variation of the current with the voltage can be modelled by a serial resistance called “R_S”. $V_{Threshold}$ can be

Table 1
Advantages and disadvantages of different materials considered for the fabrication of micropyrotechnical systems

Micromachining technology	Advantages	Disadvantages
Silicon		
Bulk micromachining	Well known technology	High thermal conductivity
Surface micromachining	CMOS compatible	
	High melting point	
Ceramic		
Dry etching	Low thermal conductivity	Difficult to integrate electrical components
Injection molding		
Glass		
Wet etching	Low thermal conductivity	Low melting point (Pyrex, Foturan)
Dry etching		Limited 3D machining

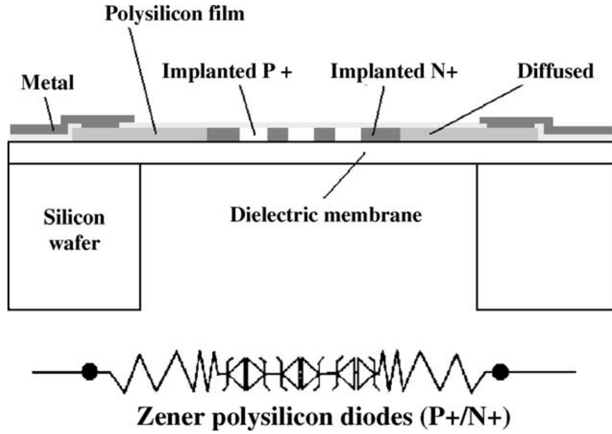

Fig. 4. Elementary symmetrical threshold elements cross-section and its electric schematic.

adjusted to a lower value by reducing the number of polysilicon diodes or increasing the doping level of the N^+ implanted zone.

For the ignition, we exploit the thermal dissipation generated by the current passing through the Zener polysilicon diodes and in the resistive part (R_S). Therefore, addressing an array of heaters with symmetrical threshold elements is based on the difference between $V_{Threshold}$ and $3 \times V_{Threshold}$ instead of on an absolute value of $V_{Threshold}$. Any modification in the $V_{Threshold}$ value induces a proportional evolution of all the others guarantying the functionality of the addressing even if the range of the applied voltage is changed. Therefore, with this technology, the most important parameter is the good homogeneity of $V_{Threshold}$ in the array, and not the $V_{Threshold}$ absolute value.

The parasitic circuit can be modelled as three groups (G1, G2, G3) of symmetrical threshold elements in series. The G1 group is constituted by all the cells of the same line as the selected one. The G3 group is constituted by all the other cells of the selected row. The others cells (other lines, and other rows) are the G2 group. As there are three groups in series, between $V_{Threshold}$ and $3 \times V_{Threshold}$, the parasitic current is reduced (cf. graph of Fig. 5) and 99.9% of the applied power is dissipated in the selected thruster.

4. Review of the fabrication processes

4.1. The matrix of addressable heating elements

A 4 in. 350 μm thick silicon wafer is thermally oxidized. Then, the wafer is coated with silicon rich low pressure chemical vapor deposition (LPCVD) nitride. The resulting thickness is of 2 μm. In a third step, a layer of 0.5 μm of polysilicon is deposited by LPCVD at 605 °C. This polysilicon film is doped N^+ by an arsenic implantation ($N_D = 5.10^{18}\ \mathrm{cm}^{-3} \Rightarrow R_\square = 500\ \Omega/\square$). Then, the polysilicon film is etched by reactive ion etching (RIE) to pattern the igniter's shape. The film is doped P++ by a Boron implantation ($N_A = 1.10^{20}\ \mathrm{cm}^{-3} \Rightarrow R_\square = 30\ \Omega/\square$) only on selected parts with a photoresist mask (cf. Fig. 6a). This P++ implantation permits to create the N+/P++ junctions. The selected heater zone is then protected by a PECVD oxide and the non protected polysilicon zone is then heavy doped by diffusion of phosphorus ($N_D > 10^{21}\ \mathrm{cm}^{-3} \Rightarrow R_\square = 20\ \Omega/\square$). Next steps are the deposition of a passivation layer (SiO_2), the contact opening and the Al metallization. Final step is the back side deep reactive ion etching (DRIE) to liberate the membrane. The process steps are summarized in Fig. 6b.

Several arrays have been thus processed. Fig. 7 gives photos of realizations: (a) is an elementary polysilicon threshold element, (b) is a back side view of nine cells where we can distinguish the polysilicon element by transparency and (c) is a photo of the entire array of 100 elements where 40 contacts are visible (only 20 are used).

4.2. The chambers matrix

Two chambers materials have been considered to serve as propellant tank: silicon and Foturan. On one hand, the main advantages of using silicon lie in the existence of highly developed and controlled fabrication processes and in its high melting point. Moreover, the realization of the microthrusters parts using only silicon would minimize the thermal expansion mismatch between the materials. On the other hand, Foturan offers a lower heat conductivity that can result in a better thermal insulation between the chambers, which could be of importance when con-

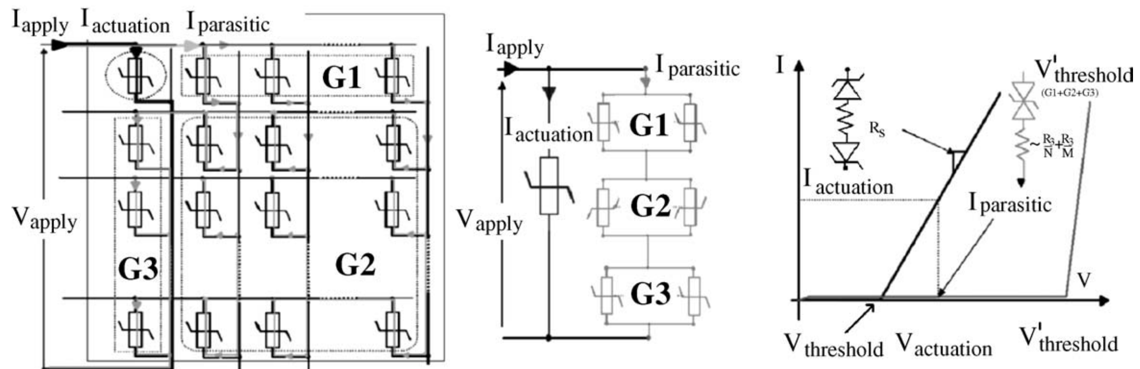

Fig. 5. Addressable array and equivalent electrical model. I_{apply} is the applied current to the complete array. V_{apply} is the applied voltage to the complete array. $I_{actuation}$ is the part of the applied current flowing through the selected thruster. $I_{parasitic}$ is the part of the applied current lost in the non selected thrusters. $I_{apply} = I_{actuation} + I_{parasitic}$. $V'_{Threshold}$ is the threshold voltage of the parasitic circuit (non selected thruster), $V'_{Threshold} = 3 \times V_{Threshold}$.

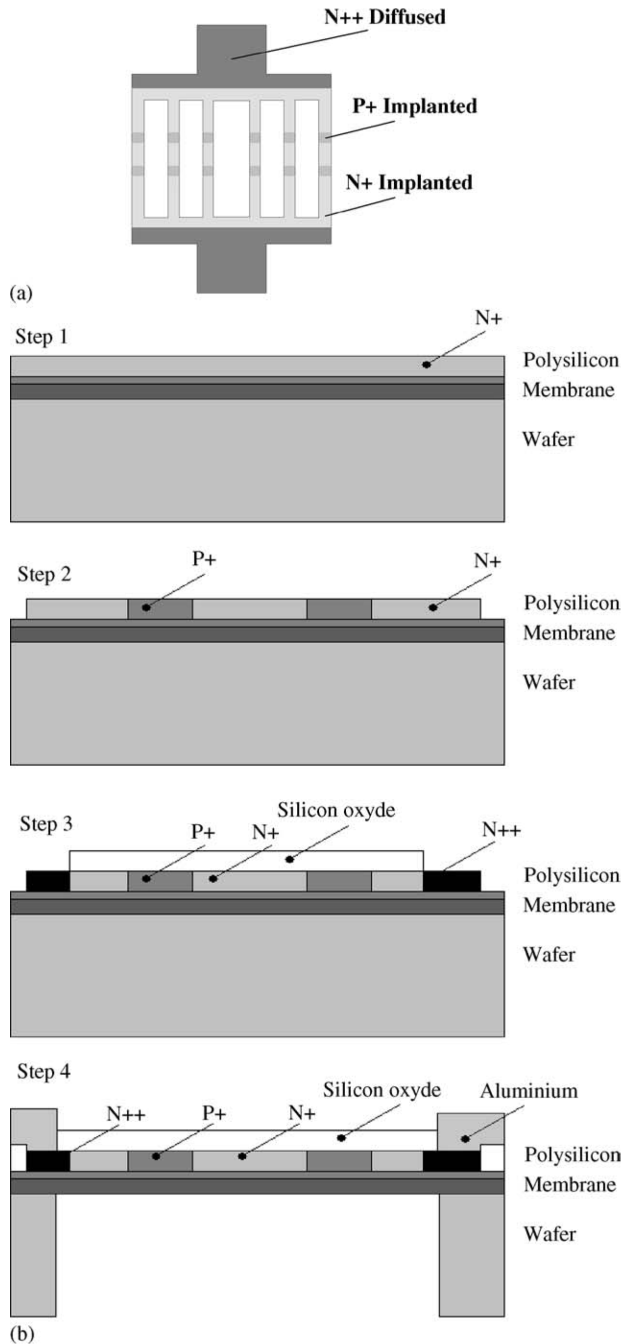

Fig. 6. (a) Layout of one threshold element. (b) Addressed igniters' array main process steps.

sidering the thermal crosstalk between a single thruster and its closest neighbours [8].

4.2.1. *Silicon chambers*

The silicon chambers are realized by deep reactive ion etching of silicon, using the Multiplex ICP (ASE HR) with the Bosch process [21] from Surface Technology Systems (STS). Chambers with an area of 1.5 mm × 1.5 mm are etched through in 525 μm and 1 mm thick double side polished silicon wafers. A thick thermal oxide and a thick photoresist are used as mask. In the case of 1 mm-thick wafers, they are etched in two steps. A double side photolithography is used to pattern both the top and backside of the wafer. First, from the topside, the silicon wafer is etched to about 575 μm deep. Then the wafer was turned over and the silicon wafer was etched through from the backside. Since a complete combustion could not be obtained (see Section 5.3) using chambers separated by 1 mm-thick silicon walls, thermal insulating grooves were also implemented to decrease the heat loss paths and evaluate their effect on the thermal crosstalk between neighbouring cells during the propellant combustion. The width of the grooves was of 250 μm and 500 μm with, respectively, 100 μm and 50 μm wide Si arms holding the different chambers together (Fig. 8).

Due to the aspect ratio dependent etching rates of DRIE [22], a special mask design is used to through-etch the narrow grooves without over etching the wide chambers. It consists of etching the perimeter of the structures with a trench. When the etching reaches the bottom of the wafer, the chamber middle piece becomes separated from the bulk of the wafer, as illustrated in Fig. 9. Since the trench width corresponds to the insulating grooves dimension, all structures are etched at the same rate and no significant over etching is noticed.

Arrays of chambers were etched in 1 mm-thick silicon wafers using the described double side DRIE process (Fig. 10). Anodic bonding of a 300 μm thick Pyrex wafer was used to seal the chambers on one side. Another way of proceeding to avoid any silicon interconnections between the chambers walls would have been to anodically bond the Pyrex wafer on the silicon and etch the silicon wafer afterwards.

4.2.2. *Foturan chambers*

Foturan is a photostructurable glass from Schott that can be anisotropically wet etched. The Foturan wafers used were 1 mm-thick and each fabricated chambers covered an area of 1.5 mm × 1.5 mm. The glass was exposed to UV light through an aluminium thin film mask in which the structures were previously patterned. After the removal of the aluminium layer, a heat development step was performed using temperature ramps with plateaus at 510 °C and 595 °C. During this heating step, the exposed glass crystallized around the silver atoms whereas the unexposed parts stayed in their glassy form. Finally, the etching of the exposed areas, which presented an etch rate about 20 times higher than that of the vitreous region, was done in a 10% solution of hydrofluoric acid at room temperature using an ultrasonic bath. When making chambers closed on one side, the etched cavities had a non uniform profile at the bottom and variable thicknesses, even though the surface to be etched faced the bottom of ultrasonic bath to help the evacuation of the etched material. Therefore, through-wafer holes were etched from the top and backside of the glass wafer at the same time. The influence of the position of the wafer in the ultrasonic bath was investigated and the evaluation of the results showed that different wall profiles could be obtained. The topside is defined as the side that faced towards the lamp during the UV exposure. Arrays of 100 chambers have been fabricated in 1 mm-thick Foturan wafers with the topside of the wafer placed upside down in the ultrasonic bath to minimize the curvature of the walls and the non uniform widening of the chamber dimensions (Fig. 11a).

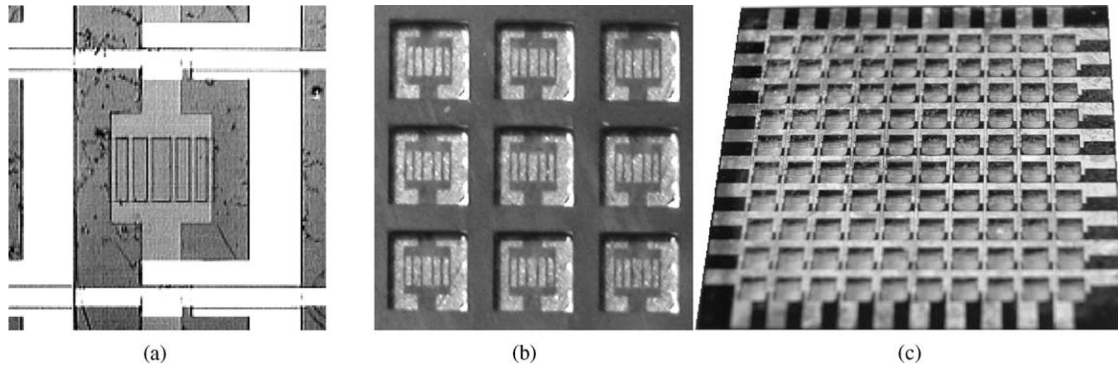

Fig. 7. Photos of realizations: (a) elementary cell, (b) back side view of nine cells, (c) entire matrix topside view.

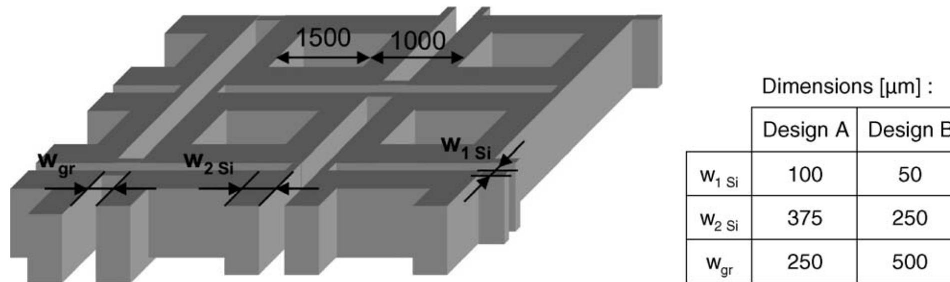

Dimensions [µm] :

	Design A	Design B
$w_{1\ Si}$	100	50
$w_{2\ Si}$	375	250
w_{gr}	250	500

Fig. 8. Schematic view of the design of the chambers with the insulating grooves.

The widening of the structures could be compensated by an appropriate mask design. The fabricated chambers exhibited a negative wall profile with an angle of 2–3° as reported in [23] (i.e. the chamber backside is larger than the topside, Fig. 11b). The thickness of the wafer was also affected by the etching process; a reduction of 100–150 µm of the wafer thickness was measured. A polishing step should be performed to have reservoirs with a reproducible volume of propellant. The optimization of the pro-

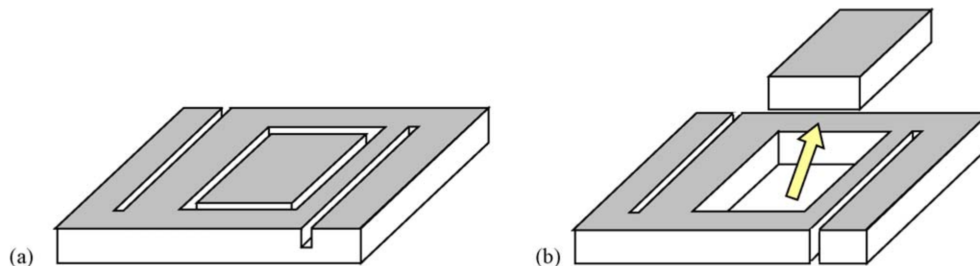

Fig. 9. Chambers and grooves etching principle: (a) the grooves and chambers outline are etched, (b) the wafer is through-etched and the silicon piece in the middle of the chamber comes off.

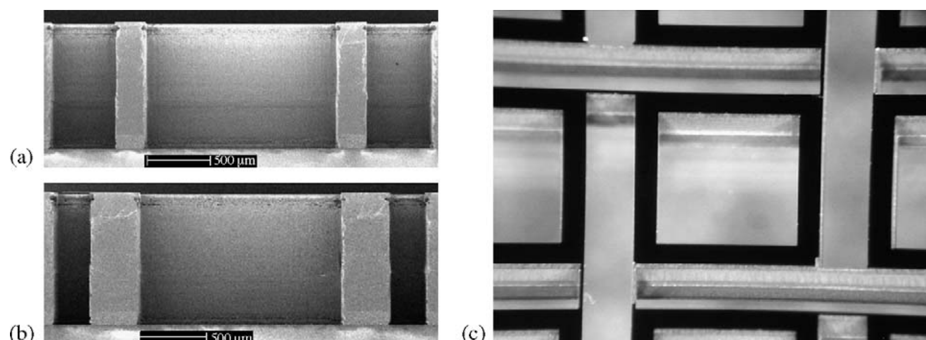

Fig. 10. Cross-section of 1.5 mm × 1.5 mm chambers with (a) the 500 µm-wide grooves, (b) the 250 µm-wide grooves etched by DRIE in a 1 mm-thick Si wafer and sealed by the anodic bonding of a Pyrex wafer, (c) Top view of the chambers array.

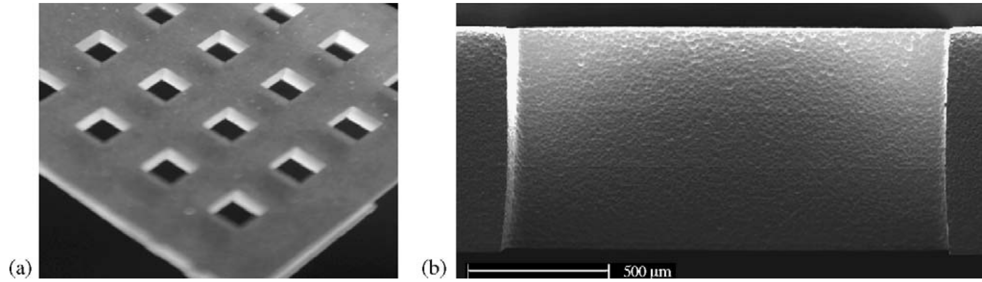

Fig. 11. (a) Photo of the Foturan chip, (b) SEM cross-sections of Foturan chambers made with the wafer with the UV exposed face up in the ultrasonic bath.

cess could include the control of the intensity of the UV light exposure and the use of a laser instead of lamp or modified mask patterns [24].

4.3. The nozzles matrix

The design of the nozzle consists of a cavity, a throat and a diverging part (Fig. 2). The 50 μm deep cavity (1.5 mm × 1.5 mm) prevents the membrane of the igniter to touch the nozzle part when bending during the ignition process. To develop the fabrication process, the target value for the angle α has been set to 10°. DRIE was investigated to etch holes with inclined walls in silicon. The number of silicon etching steps needed is reduced to two. Circular holes were dry etched through a silicon wafer. Deep reactive ion etching of silicon, using the Multiplex ICP (ASE HR) with the Bosch process from Surface Technology Systems was used. A process was developed to obtain walls with a negative angle to form the diverging part of the nozzle. Then from the same side, the silicon wafer is wet etched in KOH to structure the wide cavity. Finally, the wafer is flipped over to obtain the final structure as in Fig. 2.

The description of the fabrication process is given in Fig. 12. The sequence of the processing steps was chosen to avoid performing a photolithography on a silicon wafer with three dimensional structures. The process starts with the deposition of a 200 nm LPCVD silicon nitride on a 300 μm-thick double side polished silicon wafer. The silicon nitride film is patterned on the front side of the wafer and completely removed on the backside using reactive ion etching. The patterned silicon nitride film corresponds to the area of silicon to be wet etched and will be used later in the fabrication process to protect the silicon during the growth of a silicon oxide masking layer. A 1 μm-thick CVD silicon oxide film and a thick film photoresist (AZ-4562) are used as a mask during the conic DRIE of the silicon wafer. By varying different parameters during the DRIE process (see Table 2), such as decreasing the gas flow and increasing the power of the radio frequency coil and plate during the passivation cycles, modifying the time of the etching and passivation cycles and finally using a mix of low and high frequencies, a maximum angle of 4° was obtained. The angle is limited by the Bosch process in itself and by the mask design. Indeed, by inverting the mask polarity, the silicon plugs etched had walls with higher angle values were obtained.

Once the diverging parts are etched in the silicon wafer and the masking layers removed, a thick silicon oxide film is thermally grown. After the etching of the silicon nitride film using

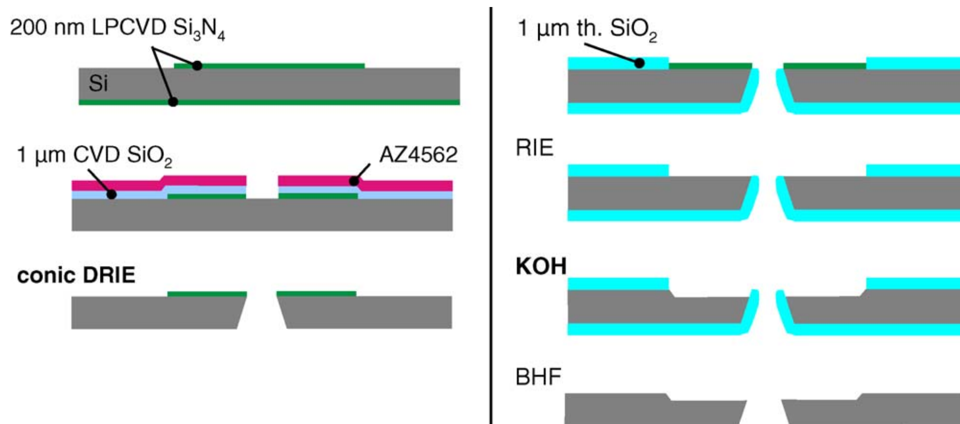

Fig. 12. Schematic description of the fabrication process of the nozzle part which includes two silicon bulk micromachining steps.

Table 2
Variation of the DRIE process parameters investigated to obtain negative conic holes (E = etching cycle, P = passivation cycle)

SF_6 (sccm)	O_2 (sccm)	C_4F_8 (sccm)	Pressure (mTorr)	RF coil E/P (W)	RF plate E/P (W)	RF plate HF/LF	Cycle E/P (s)
200–300	10	80–150	5–35	2500/800	15–30/10–20	Both	5–12/3–5

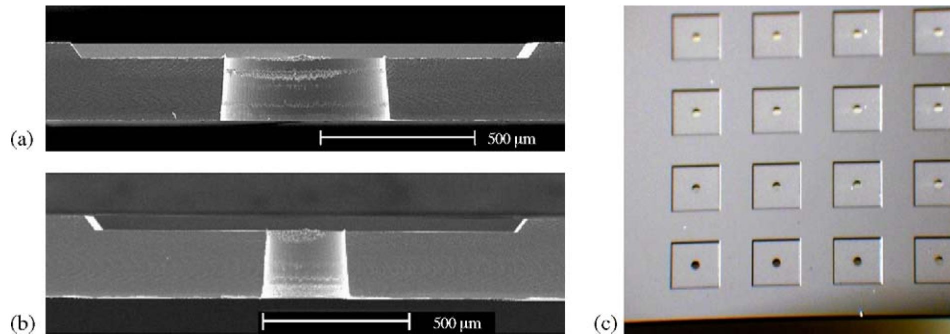

Fig. 13. Cross-section of 1.5 mm × 1.5 mm nozzles with (a) a 500 μm-wide throat, (b) a 250 μm throat etched by DRIE in a 300 μm thick Si wafer; the 50 μm-deep cavity was realized using KOH etching, (c) top view of the nozzles array.

reactive ion etching, the silicon oxide film is used as a protection during the wet chemical etching of silicon in a KOH solution (40%, 60 °C) to form the cavity used as a gap between the throat of the nozzle and the igniter membrane. Finally, the nozzle fabrication is completed by the etching of the silicon oxide left in a BHF solution. Fig. 13 presents the pictures of nozzles with two different throat diameters and of the nozzles array.

Other ways to fabricate the nozzle part using DRIE could be to reflow the photoresist to obtain a mask with a thickness gradient or to isotropicaly dry etch the silicon wafer to underetch the masking layer [25]. Micro-electro-discharge micromachining of silicon, laser etching of glass and inclined UV lithography on SU-8 are some microfabrication techniques that could be applied to fabricate a nozzle throat with the specified angle [26].

4.4. *The assembling procedure*

Because of the simplicity of the process and the propellant contamination of the surface after filling, adhesive bonding was preferred for the assembling process. A rigorous procedure using a FLIP-CHIP machine has been set up and permits to align each part at 10 μm.

First step concerns the preparation of the chamber part, part A of Fig. 14. When the chamber material is silicon, a Pyrex seal wafer is anodically bonded to the chamber wafer to receive the propellant. When the chamber material is Foturan, the Pyrex seal wafer is glued to the chamber wafer with an UV sensitive polymer (NOA 88, Norland) before receiving the propellant. The UV glue is spun-on the seal wafer. In a second step, the nozzle part is bonded to the igniter part by a thermal epoxy (H70E, Polytec) to form what called in Fig. 14, part B. The epoxy glue is deposited on the wafer between each thruster using an automatic dispensing machine that can be programmed to have the required glue thickness and width. Then, the parts A and B are filled with solid energetic material independently using a screen printing technique [20]. The injection technique principle is derived from a high accurate deposition process developed for microelectronic board industry. This technology takes a dynamic new approach to the application of solder paste for manufacturing pre-placement. The igniter and chambers' cavities are emptied from its air just before filling with propellant to ensure a good thermal contact between the propellant and the igniter's membrane (see Fig. 14).

The intermediary chamber is then glued to the filled part A with the same procedure. Finally, the two wafers stacks are again bonded together by thermal epoxy (H 70 E, Polytec). Between each step using the H70E epoxy glue, a cure at 60 °C permits the reticulation. After reticulation the H70E epoxy glue can endure ±100 °C with a no significant expansion and can be use in high vacuum (10^{-7} Torr) with no outgassing.

5. The validation tests

In this section, we present test results that validate the design, the technological choices and the fabrication processes. They include three points:

1. the validation of the addressing to be sure that only the desired thruster is ignited on the order of electronic,
2. the ignition validation by determining the power consumption and reliability,
3. the combustion validation to confirm that the combustion of the triggered thruster is sustained until the end of the reservoir and does not ignite the first level of neighbours.

The completed experimentation procedures and results have been already reported [1].

5.1. *The addressing validation*

Experiments have shown that each symmetrical threshold element could be actuated individually. Fig. 15 presents the $I(V)$ and $P(V)$ characteristics of 17 symmetrical threshold elements dispersed in the array. These measurements show an excellent reproducibility of $V_{\text{Threshold}}$ in the same array. The dispersion visible on the R_S value is principally due to the resistance through lines and rows of the farthest cells in the arrays. Considering four arrays realized from the same wafer, the I(V) characteristics are very close: the dispersion on the $V_{\text{Threshold}}$ and the R_S values are less than 2%. Considering several wafers from the same run, dispersion on the $V_{\text{Threshold}}$ and the R_S values rises up to 10% and 5%, respectively. This is due to the lack of reproducibility of the polysilicon structure. However, the most important parameter for the good functionality of the addressing being the good homogeneity of $V_{\text{Threshold}}$ in the array, the dispersion of $V_{\text{Threshold}}$ and R_S is not really a problem for us.

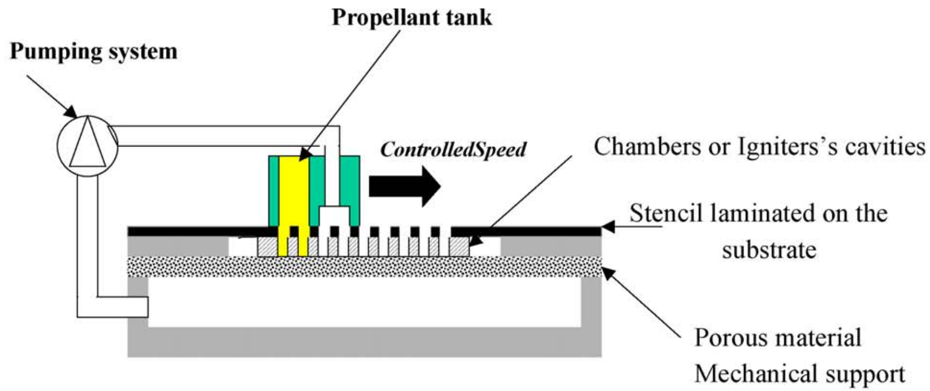

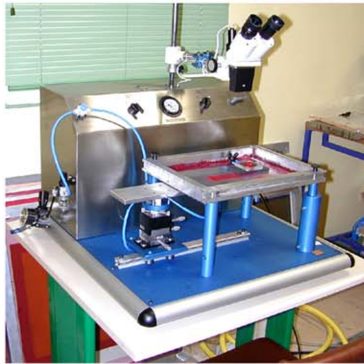

	Step	Scheme	Technique
#1	Pyrex seal / chamber assembling	chamber ⇨ part A seal	Anodic bonding or UV epoxy gluing
#2	assembling	igniter ⇨ part B nozzle	Thermal epoxy gluing
#3a	Filling with ZPP material		Manual
#3b	Filling with GAP propellant		Screen-printing under vacuum
#4	Assembling to intermediary chamber		Thermal epoxy gluing
#5	Final assembling		Thermal epoxy gluing

Fig. 14. Schematic view of the assembling procedure.

$V_{\text{Threshold}}$ can be adjusted to a lower value by reducing the number of P+ zones or also increase the doping of the N^+ implant zone.

Before filling the igniters' array with the ZPP, thermal tests have been performed using a infrared camera. Individual cells have been powered with 350 mW. Fig. 16a shows that the hot zone is well localized on the powered cell. Neighbours are non active as it can be noted on the partial view of the array (only 6×6 cells viewable). The Fig. 16b shows that the active polysilicon implanted zone (represented by the white rectangle) does not have the same emissivity as the rest of the polysilicon zone constituted of phosphorous diffused polysilicon. So, the contrast given by infrared measurements cannot be easily correlated to a thermal contrast. However, this infrared view permits to

Table 3
GAP combustion rate as function of the material used for the reservoir and measured thrust range

Chamber's material	Silicon with 250 μm grooves	Silicon with 500 μm grooves	Foturan
Mean burning rate (mm/s)	(1.3–0) Combustion not sustained	2.1 ± 0.7	2.8 ± 0.7
Thrust	–	–	0.3–2.3 mN

affirm that the localized junction's zones contribute to the global heating.

5.2. The ignition tests

Several arrays of thrusters have been filled with propellants and assembled, following the procedure of Fig. 14. The measured ignition energy using addressing polysilicon elements is of 27–48 mJ. This is the double of the ignition energy for the same material with non addressed a polysilicon heater [1]. Without the intermediary chamber between the igniter and chamber, ignition rate are very low: <3%. The main ignition cause of failure is the too early rupture of the membrane. When the pyrotechnical substance in contact with the resistor begins to heat (even below its ignition temperature), gases are released breaking the membrane before ignition is sustained. Adding an intermediary volume of air permits to absorb the overpressure between the membrane and the non ignited propellant. Even if this element presents the disadvantages to heavy the device and add one step in the assembling process, it permits to improve greatly the ignition success that reaches 100%.

5.3. The combustion tests

When silicon is used for the chamber without adding insulation grooves between each thruster, the heat generated by the combustion of the propellant ignites its first neighbours and then nearby close neighbours as close neighbours, it is propagated to all the thrusters. For silicon with the air grooves of 250 μm, the propellant combustion starts, sustains a little, then stops in the reservoir before its entire completion. For grooves of 500 μm, combustion propagates in the entire chamber and no undesired neighbours ignition occurs. Tests with Foturan chamber, showed that the GAP burns at a constant rate in the entire chamber. Burning rates are reported in Table 3. Results showed that, due to its very low thermal conductivity, Foturan is the best material for the realization of combustion chamber. Table 2 also gives the measured thrust range for thruster with Foturan chamber. 0.3 mN and 1.3 mN correspond to the thrust values for thruster without nozzle and with a Ø 250 μm throat nozzle, respectively.

6. Conclusion

In this paper, we have reported the final achievements of Micropyros project concerning the technological development. An array of 100 addressed microthrusters have been successfully fabricated, assembled and tested. It contains three main micromachined layers: the first silicon layer contains the micronozzles; the second silicon layer holds the addressing and heating elements; the third layer, in photoetchable glass or silicon, holds the propellant reservoirs. An intermediary silicon chamber is added between the igniter part and the propellant: it permits to reach 100% of ignition success and a reliable flame transition between the igniter to the propellant contained in the chamber (100% of success).

The paper reviewed the fabrication process for each part of the device and detailed the thrusters' addressing technology based on the realization of arrays of polysilicon threshold elements. The fabrication process based on robust MEMS technologies have been developed and validated. The assembling is based on a gluing method. A rigorous procedure using a FLIP-CHIP machine has been set up and permits to align each part with a precision of 10 μm. Two different safe energetic materials have been chosen: a sensitive and energetic substance, ZPP, has been used in the igniter part to lower the ignition energy. Power required for each addressing and ignition is of 250 mW which is fairly low. A GAP based propellant is used for the chamber. The limitation of this propellant is its limiting operating sizes which is about Ø 800 μm–1 mm. Indeed, for a section of combustion lower than 1 mm^2, the combustion does not sustain. That is why a new recent trend is to develop new materials with « tailored » performances: not very sensitive to shocks and friction, but containing sufficient energy to support combustion despite very small dimensions. No doubt this is the way that will be followed for applications in the future.

To conclude, the Micropyros fabrication processes quality has been validated for any future solid chemical propulsion system having the following range of dimensions: chamber diameter or width in the range of 1–5 mm and length in the range of 1–5 mm. The addressing technology has been demonstrated for a 100 elements array but can be implemented for any dimensional arrays, the limitation being the size of the silicon wafer used for the fabrication.

References

[1] C. Rossi, B. Larangot, A. Chaalane, D. Lagrange, Final characterizations of millimeter scale pyrotechnical microthrusters, Sens. Actuators A 121 (2) (2005) 508–514.
[2] E.B. Rudnyi, T. Bechtold, J.G. Korvink, C. Rossi, Solid Propellant Microthruster: Theory of Operation and Modeling Strategy, in: Proceedings of the AIAA Nanotech 02 Conference, Houston, USA, September 9–11, 2002.
[3] J. Palacin, M. Salleras, M. Puig, J. Samitier, S. Marco, Evolutionary algorithms for compact thermal modelling of microsystems: application to a micro-pyrotechnic actuator, J. Micromech. Microeng. 14 (2004) 1074–1082.
[4] C. Rossi, D. Estève, N. Fabre, T. Do Conto, V. Conédéra, D. Dilhan, Y. Guélou, A new generation of MEMS based microthrusters for microspacecraft applications, in: Proceedings of the Micro and Nano Technology for Space Applications (MNT'99), Pasadena, USA, April 1999, pp. 10–15.

[5] D.H. Lewis Jr., S.W. Janson, R.B. Cohen, E.K. Antonsson, Digital micro-propulsion, Sens. Actuators A 80 (2) (2000) 143–154.
[6] K.L. Zhang, S.K. Chou, S.S. Ang, Development of a solid propellant microthruster with chamber and nozzle etched on a wafer surface, J. Micromech. Microeng. 14 (2004) 785–792.
[7] D.W. Youngner, S.T. Lu, E. Choueiri, J.B. Neidert, R.E. Black JIII, K.J. Graham, D. Fahey, R. Lucus, X. Zhu, MEMS megapixel micro-thruster arrays for small satellite station keeping, in: 14th Annual AIAA/USU Conference on Small Satellite Logan, Utah (USA), Août 2000, pp. 21–24.
[8] B. Larangot, C. Rossi, T. Camps, A. Berthold, P.Q. Pham, D. Briand, N.F. de Rooij, M. Puig-Vidal, P. Miribel, E. Montané, E. López, J. Samitier, Solid Propellant Micro-rockets—Towards a New Type of Power MEMS, in: Proceedings of the AIAA Nanotech 02 Conference, Houston, USA, September 9–11, 2002.
[9] K. Takahashi, H. Ebisuzaki, H. Kajiwara, T. Achiwa, K. Nagayama, Design and Testing of Mega-bit Microthruster Arrays, in: Proceedings of the AIAA Nanotech 02 Conference, Houston, USA, September 9–11, 2002.
[10] G. Lamedica, M. Balucani, A Ferrari, P.D. Tromboni, M. Marchetti, Microthruster in silicon for aerospace application, IEEE AESS Systems Magazine (2002) 22–27.
[11] B.S. Tanaka, R. Hosokawa, S. Tokudome, K. Hori, H. Saito, M. Watanabe, M. Esashi, MEMS-based solid propellant rocket array thruster with electrical feedthroughs, Trans. Jpn. Soc. Aeronautical Space Sci. 46 (2003) 47–51.
[12] Y. Zheng, Z. Gaofei, L. Baoxuan, H. Songqi, Design, fabrication and test of MEMS propulsion with solid propellant, in: Proceedings of the 4th Round Table on Micro/Nano Technologies for Space, ESA-ESTEC, May 2003.
[13] P.Q. Pham, D. Briand, C. Rossi, N.F. De Rooij, Downscaling of Solid Propellant Pyrotechnical Microsystems, Tech. Digest Transducers'03, Boston, USA, June 8–12, 2003, pp. 1423–1426.
[14] B. Larangot, C. Rossi, A. Chaalane, H. Granier, P.F. Calmon, Ignition and combustion investigation on pyrotechnical solid microthruster, in: Proceedings of the 17th European Conference on Solid-State Transducers (EUROSENSORS XVII), Guimarães, Portugal, September 21–24, 2003, pp. 744–747.
[15] C. Rossi, Evaluation of Solid Propellant Technology for Small Satellite Station Keeping, LAAS internal report No. 02263—ESA–ESTEC contract report 15845/01/NL/PA.
[16] http://www.imtek.uni-freiburg.de/simulation/benchmark/.
[17] A.N. Ali, S.F. Son, M.A. Hiskey, D.L. Naud, Novel high nitrogen propellant use in solid fuel micropropulsion, J. Propul. Power 20 (1) (2004) 120–126.
[18] H.H. DiBiaso, B.A. English, M.G. Allen, Solid-phase conductive fuels for chemical microactuators, Sens. Actuators A 111 (2–3) (2004) 260–266.
[19] K. Engelen, M.H. Lefebvre, Properties of gas-generating mixtures related to different fuel and oxidizer composition, Propellant Explosives Pyrotechnics 28 (4) (2003) 49–76.
[20] Patent FR2845858, Dispositif de remplissage de zone ouvertes situées en creux par rapport à une surface.
[21] F. Lärmer, A. Schilp, Robert Bosch GmbH, Patents 4241045C1 (DE), 4855017 and 4784720 (USA).
[22] J. Kiihamäki, S. Franssila, J. Vac. Sci. Technol. A17 (4) (1999) 2280.
[23] H. Becker, Sens. Actuators B 86 (2002) 271.
[24] U. Brokmann, Microsystems Technol. 8 (2002) 102.
[25] A. Bertz, M. Kuchler, R. Knofler, T. Gessner, A novel high aspect ratio technology for MEMS fabrication using standard silicon wafers, Sens. Actuators A (97–98) (2002) 691–701.
[26] M. Han, W. Lee, S.-K. Lee, S.S. Lee, 3D microfabrication with inclined/rotated UV lithography, Sens. Actuators A 111 (2004) 14–20.

Biographies

Dr. Carole Rossi received her physics engineering degree from the National Institute of Applied Sciences in Toulouse, France in 1994. She received her PhD degree in electrical engineering and physics in 1997 from the same Institute. Currently she is a researcher at the French National Center for Scientific Research (CNRS) and she is working at LAAS (Laboratory for Analysis and Architecture of the Systems) in the Microsystems group. Her current research focuses micro pyrotechnical systems as solid propellant microthruster, pyrotechnical microactuator for microfluidics application.

Maxime Dumonteuil was born on 20 January 1977. He received a Master's degree in physics in 2002 at the University of Paul Sabatier (Toulouse, France). He is preparing a PhD thesis in Microsystems and Integration of Systems at LAAS-CNRS. He is working on the conception and realization of addressing system for microheaters application.

Thierry Camps was born in 1964. He received his Master's degree in microelectronics in 1987 and his PhD degree in electronic engineering in 1991 from the University of Paul Sabatier (Toulouse, France). The PhD thesis was prepared at the Laboratory for Analysis and Architecture of Systems, French National Center of the Scientific Research (LAAS-CNRS). The topic of the thesis was the conception, realization and characterization of "Power HBT" on GaAs. Now, his current research focuses on microsystems addressability (thermal actuators) and thermal management for microfluidics applications.

Dr. Danick Briand received his BEng degree and MASc degree in engineering physics from École Polytechnique in Montréal, Canada, in collaboration with the Laboratoire des Matériaux et du Génie Physique (INPG) in Grenoble, France, in 1995 and 1997, respectively. He obtained his PhD degree in the field of micro-chemical systems from the Institute of Microtechnology, University of Neuchâtel, Switzerland in 2001, where he is currently a team leader. He is incharge of European and industrial projects, of the supervision of doctoral students and he is involved in the educational program. His research interests in the field of microsystems include wafer bonding, PowerMEMS, polymeric MEMS, the integration of nanostructures on microsystems and the integration, packaging and reliability of micro-chemical sensors.

Phuong Quyên Pham received her MS degree in microengineering from the Swiss Federal Institute of Technology Lausanne (Ecole Polytechnique Fédérale de Lausanne, EPFL) in 2001. She is currently pursuing the PhD degree at the Institute of Microtechnology of the University of Neuchâtel, Switzerland, where she is working on pyrotechnical powerMEMS.

Prof. Nicolass F. de Rooij received a PhD degree from Twente University of Technology, The Netherlands, in 1978. From 1978 to 1982, he worked at the Research and Development Department of Cordis Europa N.V., The Netherlands. In 1982, he joined the Institute of Microtechnology of the University of Neuchâtel, Switzerland (IMT UNI-NE), as professor and head of the Sensors, Actuators and Microsystems Laboratory. Since October 1990 till October 1996, he was acting as director of the IMT UNI-NE. Since 1987, he has been a lecturer at the Swiss Federal Institute of Technology, Zurich (ETHZ), and since 1989, he has also been a professor at the Swiss Federal Institute of Technology, Lausanne (EPFL). His research activities include microfabricated sensors, actuators and microsystems.